SAND2015-8668C

Understanding the Risk of Chloride Induced Stress Corrosion Cracking of Interim Storage Containers for the Dry Storage of Spent Nuclear Fuel: Residual Stresses in Typical Welded Containers

D.G Enos[1], C.R.Bryan[2]
[1]Materials Reliability Department
[2]Storage and Transportation Department
Sandia National Laboratories
Albuquerque, NM 87185

ABSTRACT

The majority of current dry storage systems used for spent nuclear fuel consist of a welded 304 stainless steel container placed within a passively-ventilated concrete or steel overpack. In service, atmospheric salts, a portion of which will be chloride bearing, will be deposited on the surface of these containers. As the canister surface cools over time, these salts will deliquesce to form potentially corrosive chloride-rich brines. Because austenitic stainless steels are prone to chloride-induced stress corrosion cracking (CISCC), the concern has been raised that SCC may significantly impact long-term canister performance. While the susceptibility of austenitic stainless steels to CISCC is well known, uncertainties exist in terms of the residual stress states that will exist at the container welds. A full-scale cylindrical mock-up was produced, and the residual stresses associated with the weldments in that structure characterized. Results to date indicate that residual stresses will be large and tensile in both the axial and hoop directions, extending through the thickness of the container wall.

INTRODUCTION

Following initial cooling in pools, spent nuclear fuel (SNF) is transferred to dry storage casks for longer-term storage at the reactor sites. The storage cask systems are predominantly welded stainless steel (Hanson et al. 2012) containers enclosed within a ventilated concrete or steel overpack. These cask systems are intended as interim storage until a permanent disposal site is developed, and until recently, were licensed for up to 20 years, and renewals also up to 20 years. In 2011, 10 CFR 72.42(a) was modified to allow for initial license periods of up to 40 years, and also, license extensions of up to 40 years. However, as the United States does not currently have a final disposal pathway for SNF, these containers may be required to perform their waste isolation function for many decades beyond the original design intent. Several recent analyses (NWTRB 2010b; EPRI 2011; Hanson et al. 2012; NRC 2012a) have identified and prioritized concerns with respect to the safety performance of long-term interim storage. In each of these studies, the potential for canister failure by chloride-induced stress corrosion cracking (CISCC) was identified as the major concern with respect to canister performance.

In those analyses, the potential for SCC of welded stainless steel interim storage containers for SNF was also identified as a high priority data gap. Uncertainties exist both in the understanding of the

environmental conditions on the surface of the storage canisters and in the textural, microstructural, and electrochemical properties of the storage containers themselves. The canister surface environment is currently being evaluated by Sandia and EPRI (Enos et al. 2013; Bryan and Enos 2014; EPRI 2014; Bryan and Enos 2015); however, little has been done to assess canister material properties and their impact on corrosion. Of specific interest are weld zones on the canisters, because the welding process modifies the microstructure of the stainless steel as well as its resistance to localized corrosion. In addition, welding introduces high tensile residual stresses that can drive the initiation and growth of SCC cracks. In order to meet the need for additional data on the canister material properties, a full-diameter cylindrical mockup of a dual-certified 304/304L stainless steel (SS) storage canister was produced using the same manufacturing procedures as fielded SNF fuel interim storage canisters. The weld and base metal zones on this mockup will be characterized to determine residual stresses, metal properties and susceptibility to SCC.

Stress corrosion cracking is a localized corrosion phenomenon by which a through-wall crack could potentially form in a canister outer wall over time intervals that are shorter than possible dry storage times. In order for SCC to occur, three criteria must be met: there must be an aggressive chemical environment present, the metal must be susceptible to SCC, and sufficient tensile stress must be present to support SCC. In general, these criteria are expected to be met, at least at some Independent Spent Fuel Storage Installation (ISFSI) sites, during the period of interim storage.

Aggressive chemical environment: Field sampling of surface deposits on in-service SNF storage canisters at three near-marine ISFSI sites has been carried out over the last three years, and analyses have shown that chloride-rich salts can be present on the canister surfaces (Enos et al. 2013; Bryan and Enos 2014; EPRI 2014; Bryan and Enos 2015). Once portions of the canister surfaces cool sufficiently for these salts to deliquesce, a corrosive chloride-rich aqueous environment could potentially form.

Susceptible material: The majority of SNF dry storage casks currently in use are made from austenitic stainless steels, including 304, 304L, and 316. Should sufficient tensile stress be present, there is ample evidence that these stainless steels are susceptible to CISCC in aggressive chloride-bearing environments. SCC of 304 SS, the most widely used alloy for containers that are currently in service, occurs readily in experimental tests with deliquesced sea-salts (e.g., (Nakayama 2006; Prosek et al. 2009; Tani et al. 2009; Mintz et al. 2012; Prosek et al. 2014), and has also been observed in near-marine ambient temperature field tests and industrial sites (Kain 1990; Hayashibara et al. 2008; Kosaki 2008; Cook et al. 2011; Nakayama and Sakakibara 2013; Cook et al. 2014). However, overall susceptibility is a function of several factors, including the degree of sensitization, the degree of cold work, and the surface finish (Parrott and Pitts 2011); to date, none of these factors have been assessed for materials representative of fielded interim storage canisters. While these factors are known to affect susceptibility to SCC, they are all specific to the material and to the manufacturing processes used to fabricate the canister. In order to evaluate them, it is necessary to obtain relevant metal samples, from a canister or mockup made using the same techniques as real, in-service canisters.

Tensile stress: In order for an SCC crack to initiate, the tensile stresses in the metal must be of a sufficiently large magnitude that the threshold stress intensity value at a potential nucleation site is exceeded. In order for an initiated crack to propagate and penetrate through the container, the applied stress intensity at the crack front must be maintained above that threshold. In other words, a sufficiently large tensile stress state must exist through the entire wall thickness. Tensile stresses may be applied externally—for instance, by loading or by pressurization—but for SNF interim fuel canisters, external loads are negligible relative to the yield stress of the metal. High residual tensile stresses may be present in the metal, however, due to cold working or welding. Weld residual stresses (WRS) are generally the most important component, and are a function of many factors, including weld geometry, sample thickness, welding speed, number of passes, inter-pass temperatures, and base metal properties relative to the weld. Because of this, WRS are specific to the geometry and welding processes used, and can only be measured from an actual storage canister or a mockup made using the same procedures as the real canisters. However, WRS measurements on samples with relevant

geometries and typical welds have never been done. The NRC modeled WRS for typical canister welds using finite element methods (NRC 2013), and predicted that within the heat affected zone (HAZ) of both longitudinal and circumferential welds, sufficient tensile stresses would be present to support SCC. Moreover, they predicted that the tensile stresses would be present through the thickness of the cylinder wall, permitting full penetration over time.

EXPERIMENTAL PROCEDURE

The mock-up whose evaluation is described in this document is based upon the TransNuclear NUHOMS 24P design (Pacific Nuclear Fuel Services 1991). This container design is employed at the Calvert Cliffs nuclear power station, which was the first site surveyed by EPRI for the dust composition on the surface of the containers (Gellrich 2013). The mock-up, pictured schematically in Figure 1 below, consists of three cylindrical shells, each being 48 inches long and 67.2 inches in diameter, and having a wall thickness of 5/8 inch. Each shell was formed by cold forming a plate into a cylinder, then making a single longitudinal weld to form the cylinder. The three cylinders were then welded together to form a single large cylinder 12 feet in length with two circumferential welds. All of the welds were formed via the submerged-arc welding process and were multi-pass. Each inner-diameter weld consisted of three passes, and with one exception, each outer-diameter weld was made with four passes (the exception had 5). The inner diameter was welded first, followed by the outer diameter. Welds were made at a rate of 15 to 16 inches per minute at a voltage of 30V and current of 400A. Typical heat input was 45 kJ/in.

In addition to welds formed under nominal conditions, repairs are commonly necessary at regions along the welds where the nondestructive testing indicated that the weld did not conform to the criteria in ASME B&PVC Section III, Division 1, Subsection NB. Repair regions have been identified by numerous researchers as having dramatically elevated residual stresses when compared to unrepaired portions of a weld (Dong et al. 2002; Bouchard et al. 2005; Dong et al. 2005; Elcoate et al. 2005; George and Smith 2005; Hossain et al. 2006; Hossain et al. 2011). During fabrication of the mockup, all of the welds were subjected to a full radiographic inspection, and no weld repairs were required. However, because of the potentially important effect of weld repairs on weld residual stresses and material properties, one region on each circumferential weld was subjected to a repair procedure on the outer diameter. In these locations, the weld metal was removed locally by drilling and grinding, then that section rewelded. The repair was welded using the gas tungsten arc welding technique. Characterization of these sites will allow determination of weld residual stresses and degrees of sensitization typical of weld repair regions.

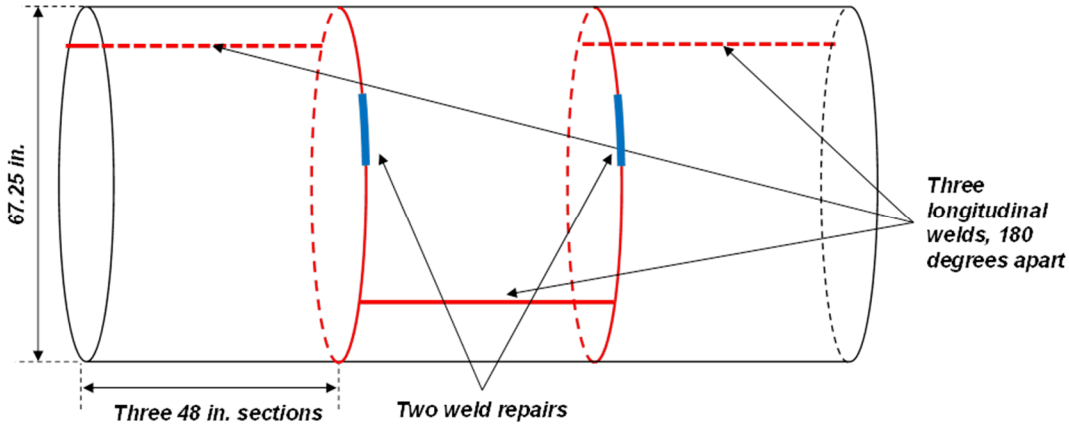

Figure 1: Schematic representation of the full scale mock storage container manufactured at Ranor

Three plates of dual-certified 304/304L stainless steel were used to construct the container. The thickness of each plate was verified via ultrasonic inspection prior to being welded. The weld filler metal was 308L SS, as typically used when welding 304. The compositions of the 304/304L plates and the 308L filler material are in Table 1 below, and indicate carbon contents below 0.03, meeting the “L”

designation. In addition to the composition of the materials of construction, the parameters for each weld pass were documented in the data package provided with the mockup. These include the current, voltage, travel speed, heat input, and interpass temperature. All welds used a double-V edge preparation with a 30 degree bevel. X-ray films of all welds and weld repairs were also included in the data package.

Table 1: Composition of 304L Plate and 308L Filler Metal Used to Construct Mock-Up

	C	Co	Cr	Cu	Mn	Mo	N	Ni	P	S	Si
Plate Material (304/304L)	0.0223	0.1865	18.1000	0.4225	1.7125	0.3180	0.0787	8.0270	0.0305	0.0023	0.2550
Weld Filler (308L) (lot 1)	0.014	--	19.66	0.16	1.70	0.11	0.058	9.56	0.025	0.010	0.39
Weld Filler (308L) (lot 2)	0.012	--	19.71	0.192	1.730	0.071	0.053	9.750	0.024	0.012	0.368

A variety of hole-drilling based techniques are available for the evaluation of the stress state in a metal sample. Typically, these techniques involve the attachment of strain gauges to the surface of the material being measured, which are monitored while a hole is precisely drilled in the material. As the hole is drilled in depth increments, the local constraint within the structure is relaxed, allowing stress relaxation to occur, resulting in surface deformation which is captured by the strain gauges. This method is known as incremental center-hole drilling (iCHD). A similar drilling technique involves the use of a surface strain gauge around which a core is cut into the material, allowing the center pillar to relax. These techniques, while they can be accurate, are only sensitive to the near-surface stresses in the material.

The deep hole drilling methodology differs from other hole-drilling techniques in that it does not rely on the use of surface strain gauges. A small diameter hole is precisely drilled via a gun drill through the material. An air gauge is then used to precisely characterize the diameter of the hole along its length. Next, electric discharge machining (EDM) is used to cut an overcore around the aforementioned hole. As the core is cut, the constraint placed on the metal immediately adjacent to the central hole is relaxed, resulting in local lateral displacement of the material. The inner diameter of the hole is then re-characterized and the resulting change in diameter, due to the loss of constraint around the hole, is recorded. From these strains, the original residual stress state within the material as a function of depth can be calculated. The deep hole drilling technique is not sensitive to near-surface stresses, and hence is commonly combined with iCHD to obtain a full through-thickness weld residual stress profile, if near-surface stresses are of interest.

The calculations used for standard deep hole drilling are based upon the assumption that the stress relaxation leading to the measured displacements is entirely elastic in nature. When large stresses are present, this is not true, and plastic deformation of the material can result, hindering the ability of the technique to resolve stress. For a heavily constrained weld, such as the circumferential weld on the interim storage containers, it is anticipated that the residual stress levels will be very high – approaching the yield strength of the material – and as such, the traditional analysis will not work. To compensate for this, the deep hole drilling technique must be modified (Mahmoudi et al. 2009; 2011). In the modified technique, the EDM core is cut in steps. After each step, the inner diameter of the hole is characterized via the air probe. By measuring the deformation of the inner diameter of the hole at the depth of the core cut, the effect of plasticity can be addressed. The resulting residual stress distribution, while being lower in vertical resolution than the traditional measurement, is able to resolve large residual stresses. This modified technique is known as incremental deep hole drilling (iDHD).

The deep hole drilling technique is semi-destructive in nature. Although a hole and EDM overbore must be drilled, the site is small (1.5mm diameter hole, 6mm diameter overbore), the remainder of the mockup will be undisturbed. Perhaps more importantly, the deep hole drilling technique can be

employed without cutting the mock-up into smaller pieces, allowing the through-wall stress profile to be measured prior to removing the cylindrical constraint on the location tested. The contour method, described below, analyzes a cross-sectional surface of the metal, which requires cutting a section of the weld from the mockup. While the use of surface strain gauges can help measure the stress relaxation associated with cutting a section from the mockup, the cutting process introduces an additional level of complexity and adds to the uncertainty of the residual stress measurement.

RESULTS AND DISCUSSION

There are two primary sources of residual stress within the container, the origin of which is best illustrated by a discussion of how the cylinder was formed. The raw material used to form each of the three segments of the cylinder was received in the form of annealed plate. These plates were then deformed into a cylinder – a process which is accomplished by gradually bending the plate, introducing significant plastic deformation of the material, and a complex stress state through the thickness of the wall. Once formed into cylinders, each plate was then welded. When the weld is made, the liquid metal in the weld pool solidifies and contracts. Since this contracting material is effectively held in place (i.e., constrained) by the overall structure of the cylinder, the degree to which the solidifying metal can contract is limited, and as a result the solidified weld and nearby heat affected zone have a considerable tensile residual stress. Similarly, the material away from the weld root is also impacted by the attempted contraction of the weld, and as a result it is under a considerable compressive residual stress. It is the combination of these two stresses (formation and welding) that forms the driving force for any potential stress corrosion cracking. When the container is subdivided by cutting, the constraint on which each portion of the container by the overall structure is changed, allowing for macroscopic deformation as the stresses relax. In order for the stresses within the as-manufactured container to be measured accurately, any such relaxation due to the cutting operation must be measured and accounted for.

Following fabrication, the mockup cylinder was cut into pieces, with one cylindrical half being retained for weld residual stress measurements. To measure any relaxation that occurred during cutting, surface-mount strain gauges were positioned along the longitudinal and circumferential welds at 10 inch intervals. While relaxation might be greater closer to the cut, the weld regions are the critical areas, as they are where WRS will be later be measured. A total of 28 strain gauges were utilized. Each strain gauge consisted of two metallic meander-path circuits oriented 90 degrees from one another and placed on a mylar backing. One of the meander paths was aligned parallel to the length of the container (denoted axial strain) and the second aligned parallel to the circumference of the cylinder (denoted hoop strain). Prior to affixing each sensor, a location was identified where there were no macroscopic scrapes/scratches present as in order to function properly, the sensor must be in intimate contact with the underlying substrate. The container surface was then cleaned using isopropyl alcohol, and an anchor pattern was applied using 240 grit SiC abrasive paper. The anchor pattern itself consisted of a cross-hatched pattern formed by using the abrasive in the lateral direction, followed by the axial direction. Once the anchor pattern was placed, the surface was cleaned again with isopropyl alcohol, after which it was etched using a mild phosphoric acid solution. Once etched, the surface was neutralized using an ammonia based solution. Next, the strain gauge was placed on a segment of gauge installation tape. The mounting surface of the gauge was then coated with an adhesion promoter, followed by a cyanoacrylate adhesive and the strain gauge was adhered to the container surface. Once the adhesive cured, leads were soldered to each of the four terminals shown in the figure. The completed gauge was then covered with a urethane coating to protect it from surface damage, and the leads secured to the surface of the container using tape.

Each strain gauge (meander path) functions as a resistor. As the surface moves due to stress relaxation, the dimensions of the strain gauge and its resistance also change. Gauges were positioned along both the circumferential and longitudinal welds as illustrated in Figure 2. In locations where the circumferential weld intersected with a longitudinal weld, three gauges were positioned as illustrated in Figure 2b. Once positioning of the sensors was complete, initial measurements were made to calibrate each of the sensors, after which the container was cut. As one of the sensors was close to the cut

region, care was taken to protect that sensor and to prevent coolant splash or tooling damage. Cutting was accomplished by positioning the container onto a rotary table and using a 1 inch roughing end mill to minimize heat input. Once cutting was complete, the sensors were monitored again, and the resulting difference in resistance transformed to an equivalent surface strain.

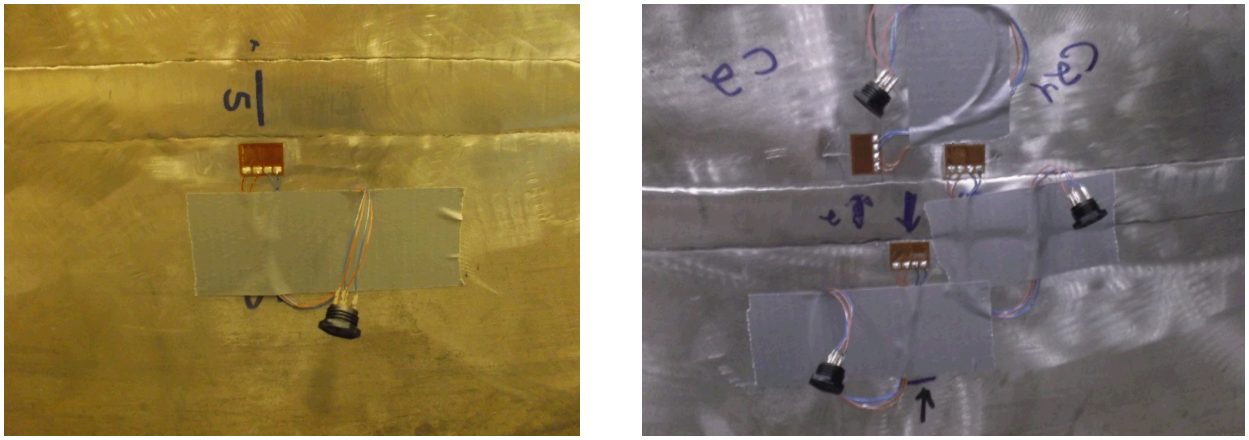

Figure 2: Surface strain gauges were positioned along the longitudinal and circumferential welds. Gauges were placed as close to the weld fusion zone as possible (a). In addition, a series of three sensors were positioned in each location where a circumferential weld intersected a longitudinal weld (b).

The surface strains measured for the circumferential weld are presented in Figure 3. In terms of their orientation, strains that are parallel with the long dimension of the container are termed “axial strains” and strains that are around the circumference/round dimension of the container are termed “hoop strains”. There are two longitudinal welds that intersect with the circumferential weld. The weld which was cut, in the middle section of the mockup (Figure 1) is termed the lower weld, and the uncut weld, in the half retained for stress measurements, is termed the upper weld.

The strains along the circumferential weld (Figure 3) were small (microstrain) and primarily tensile in nature, and represent the resolution of the technique as implemented here. At the location where the lower weld (the weld which was cut through) intersected the circumferential weld, the strains were larger, and compressive in the hoop direction (i.e., parallel to the circumference of the container), but remained tensile in the axial direction.

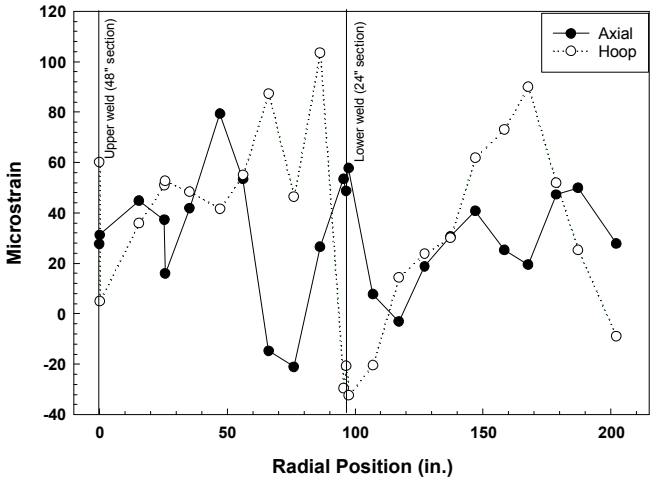

Figure 3: Surface strain measurements along the circumferential weld. Note that the sensors are located approximately 10 inches apart (with exceptions as noted above) and that the overall circumference was 211 inches (i.e., a point at 0 inches is in the same location as a point at 211 inches).

As discussed previously, sensors were placed alternately on each side of the circumferential weld. To evaluate if there was a difference between the strains experienced by the upper and lower sections, the axial and longitudinal strains were plotted as a function of which side of the weld the respective strain gauge was located. No difference was observed..

Measurements were also made along the upper and lower longitudinal welds. The data for the upper (uncut) weld is illustrated in Figure 4a. As can be seen in the figure, the strains were comparable in magnitude to those around the circumferential welds (i.e., microstrain). Strains were consistently tensile in the Axial direction and compressive in the Hoop direction. The measurements made at the lower longitudinal weld (Figure 4b) illustrate that significant deformation of the end of the container resulted from the cut. The In the longitudinal direction, the strain was tensile, while in the axial direction it was primarily compressive. This indicates that cutting the container in half resulted in a loss of constraint in the regions near the cut. As a result, the stresses from the circumferential weld (tensile hoop stress) resulted in the end of the container becoming smaller in diameter and lengthening slightly. Visually, the container could be considered to be necking down as the location of the cut is approached. Moving further from the cut, the constraint provided by the remaining structure prevented significant surface strain.

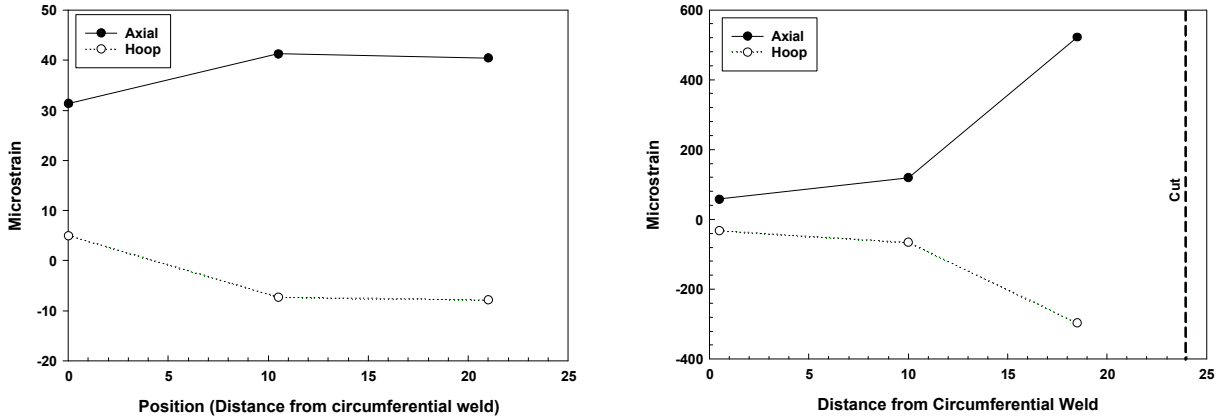

Figure 4: Axial and Hoop strains were measured along the upper (a) and lower (b) longitudinal welds. The lower weld is the one which was cut.

Residual Stress in the Base Metal

As the deep hole drilling technique is inaccurate near the outer metal surface, center hole drilling was used to measure the stresses in the first 0.5mm of material. The resulting iCHD stress distribution is shown in Figure 5a. As a point of reference, the uniaxial yield strength of annealed 304L SS is on the order of 170-200 MPa. Very near the surface, the residual stresses were tensile in nature. However, moving into the material while the axial strain remains small and tensile, the hoop stress becomes compressive in nature. The data also indicates a relatively high shear stress in the near surface region, though caution must be used when interpreting this result. In order to perform the iCHD measurements in the same location as a subsequent DHD measurement, a very small strain rosette must be used as the diameter of the hole drilled for the iCHD measurement must be smaller than that of the DHD reference hole to prevent the first measurement influencing the second. As a result, the strain gauge samples a smaller effective volume of material than would be ideal, leading to an increased signal–to-noise ratio and a corresponding increased uncertainty. Also, due to the small size of the strain gauges, any misalignment or eccentricity of the drilled hole, i.e. experimental error, will be more apparent in the results. The error bars only reflect the magnitude of the uncertainties that can be directly measured, such as curving fitting error and Young's Modulus uncertainty, and not measurement uncertainty as discussed above. As such, the data in the figure is best interpreted in terms of the average magnitude and trends, which indicates low residual stresses in the first 0.5 mm from the OD of the container.

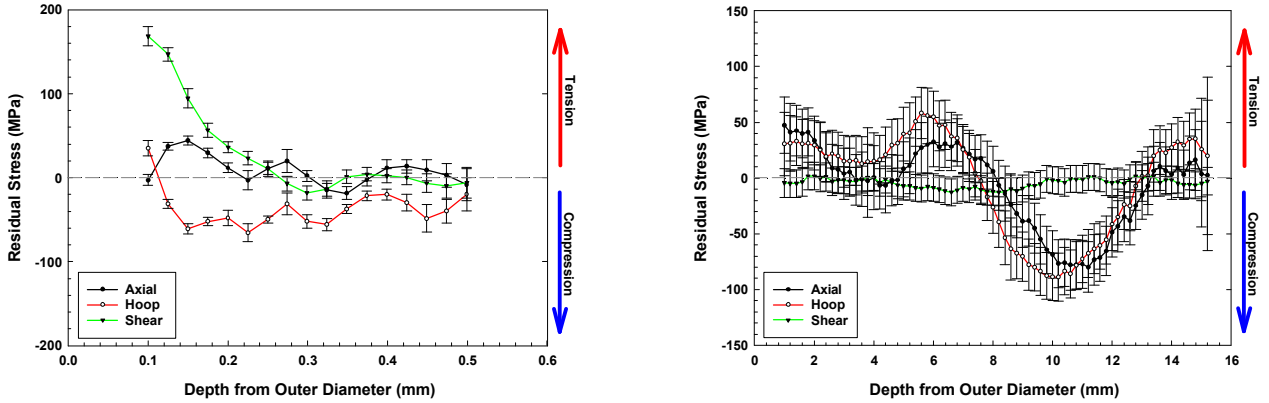

Figure 5: iCHD and DHD data as a function of distance from the outer diameter of the container for a region located far from any weldments. Note that stresses are tensile near the surfaces, then become compressive in the center of the wall due to the deformation process used to form the original plate material into a cylinder

For the stress distribution through the thickness of the container wall, deep hole drilling (DHD) was performed. Since the base metal region is far from any of the welds, the anticipated stresses are small relative to the yield strength of the material, so incremental DHD was not necessary.

The stress distribution through the container wall is shown in Figure 5b. The stress state near the outer surface of the container wall is slightly tensile in nature in both the axial and hoop directions. Moving further into the wall, the hoop stress becomes increasingly tensile, then both the hoop and axial stresses decrease to approximately zero in the center of the wall. Both the hoop and axial stresses then become large and compressive in nature until reaching the inner surface where they again become tensile in nature. The origin of these stresses is the forming process of the cylinder itself. As the plates used to manufacture the cylinder are bent, the outer diameter is placed in tension, while the inner diameter is placed in compression. In an ideal case, the stress distribution would show a uniform transition from tension to compression through the thickness of the wall. However, the formation process is not ideal, and the transformation of the plate into a cylinder is done in a stepwise fashion. Through this process, only a small portion of the plate is bent in each step, and as a result the stress state is more complex, with the bending moment only being retained in the central region of the shell.

The stress profile through the canister shell illustrates why through-thickness cracking is not anticipated at regions away from the weld. While crack initiation can take place at the surface, as the crack grows into the wall, the tensile stresses driving crack propagation will decrease, eventually becoming compressive in nature and arresting crack propagation.

Residual Stress in the Circumferential Weld (Centerline)

As discussed above, the mock storage container has two different types of welds. Due to their orientation, the welds anticipated to have the highest residual stresses are the circumferential welds, due to the constraint placed upon them by the surrounding structure. As with the base metal, iCHD was used to measure the near-surface residual stresses, the results of which are shown in Figure 6. Both the axial and hoop stresses in the near surface region are large and tensile in nature, decreasing in magnitude with depth. iDHD was used to measure the residual stresses through the thickness of the weld. In contrast to the base metal, the residual stresses in the weld root are significantly larger in magnitude, and are tensile in nature all of the way through the thickness of the container wall. As a result, if a crack were to initiate at the surface of the container, it would have a tensile stress available to support propagation through the thickness of the wall.

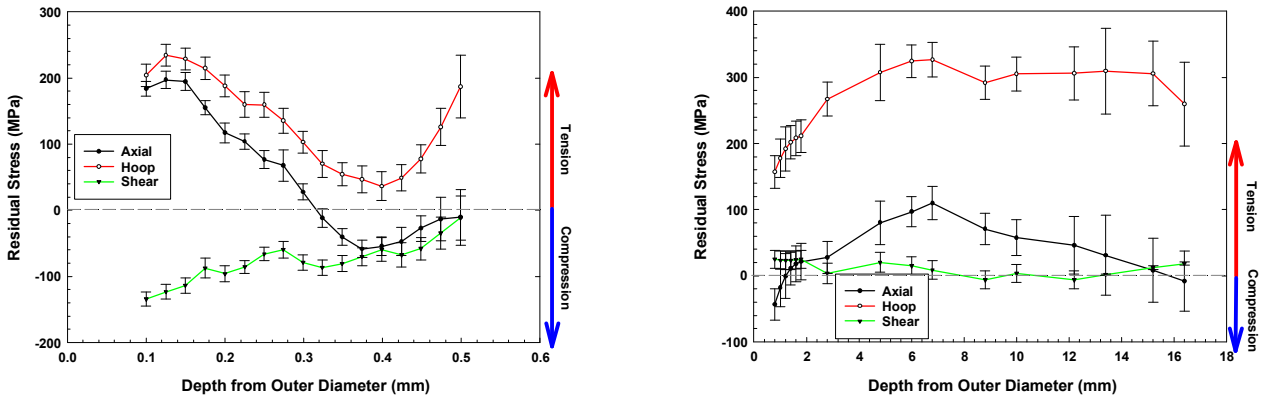

Figure 6: iCHD and DHD data as a function of distance from the outer diameter of the container for the centerline of a circumferential weld. Note that stresses are tensile through the thickness of the plate, and are largest in magnitude in the hoop direction.

Residual Stress in the Circumferential Weld (Heat Affected Zone)

While the residual stresses were anticipated to be largest in the weld fusion zone, the regions surrounding the weld (the heat affected zone or HAZ) are the regions where localized corrosion is most likely to initiate due to sensitization resulting from the thermal profile associated with the welding process. Characterization of the stresses in the HAZ was accomplished by performing iCHD and iDHD measurements approximately 4 mm from the weld toe (i.e., edge of the weld fusion zone). As with the other two locations, iCHD was used to measure the near-surface residual stresses, the results of which are shown in Figure 6. Both the axial and hoop stresses in the near surface region are large and tensile in nature, decreasing in magnitude with depth. iDHD was used to measure the residual stresses through the thickness of the weld. In contrast to the base metal, the residual stresses in the weld root are significantly larger in magnitude, and are tensile in nature all of the way through the thickness of the container wall. As a result, if a crack were to initiate at the surface of the container, it would have a tensile stress available to support propagation through the thickness of the wall.

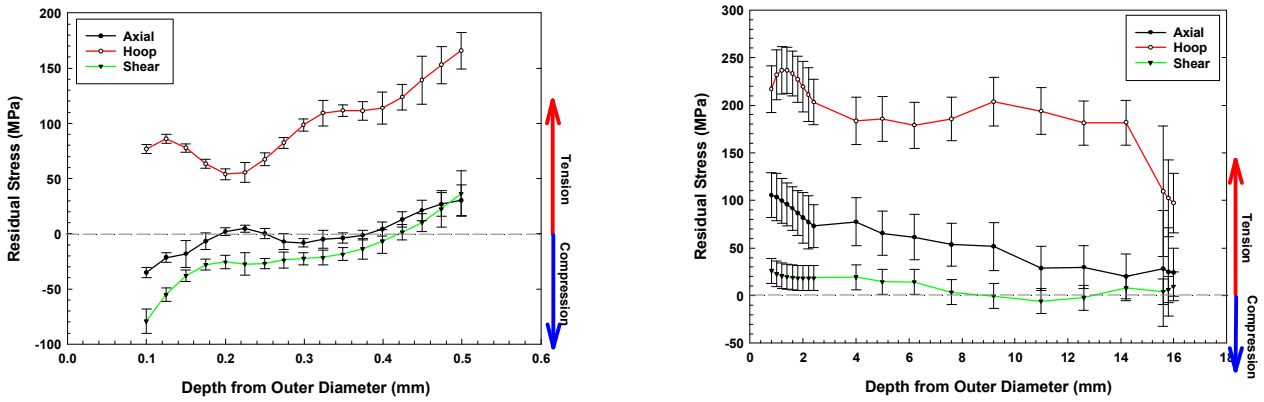

Figure 7: iCHD and DHD data as a function of distance from the outer diameter of the container for the HAZ associated with a circumferential weld. Measurements were made approximately 4mm from the weld toe. Note that stresses are tensile through the thickness of the plate, and are largest in magnitude in the hoop direction.

CONCLUSIONS

The potential for stress corrosion cracking (SCC) of welded stainless steel interim storage containers for spent nuclear fuel (SNF) has been identified as a high priority data gap by the NWTRB, EPRI, DOE, and the NRC. Uncertainties exist both in the understanding of the environmental conditions on the surface of the storage canisters, the properties of the materials used to construct the containers, and the residual stress state associated with the welds used to construct each storage container. In order to assess the residual stresses that may exist to support SCC crack propagation, a full-diameter

cylindrical mockup of a dual certified 304/304L SS storage canister was produced using the same manufacturing procedures as fielded SNF fuel interim storage canisters. The weld and base metal zones on this mockup are being characterized through deep hole drilling and other stress measurement techniques. Results to date indicate that through-thickness tensile stresses will exist at both the weld centerline and heat affected zones. However, in the base metal away from the welds (where the stress state is defined by the shaping process) residual stresses become compressive as the inner diameter of the container is approached, indicating that through-thickness cracks are unlikely in such regions.

ACKNOWLEDGEMENTS

Sandia National Laboratories is a multi-program laboratory managed and operated by Sandia Corporation, a wholly owned subsidiary of Lockheed Martin Corporation, for the U.S. Department of Energy's National Nuclear Security Administration under contract DE-AC04-94AL85000.

REFERENCES

Bouchard, P., George, D., Santisteban, J., Bruno, G., Dutta, M., Edwards, L., Kingston, E. and Smith, D. (2005). Measurement of the residual stresses in a stainless steel pipe girth weld containing long and short repairs. International Journal of Pressure Vessels and Piping 82, 299-310.

Bryan, C. R. and Enos, D. (2014). Analysis of Dust Samples Collected from Spent Nuclear Fuel Interim Storage Containers at Hope Creek, Delaware, and Diablo Canyon, California, SAND2014-16383. Albuquerque, NM. Sandia National Laboratories.

Bryan, C. R. and Enos, D. G. (2015). Analysis of Dust Samples Collected from an Unused Spent Nuclear Fuel Interim Storage Container at Hope Creek, Delaware, SAND2015-1746. Albuquerque, NM. Sandia National Laboratories.

Cook, A., Lyon, S., Stevens, N., Gunther, M., McFiggans, G., Newman, R. and Engelberg, D. (2014). Assesing the Risk of Under-Deposit Chloride-Induced Stress Corrosion Cracking in Austenitic Stainless Steel Nuclear Waste Containers. Corrosion Engineering, Science and Technology 49, 529-534.

Cook, A., Stevens, N., Duff, J., Mishelia, A., Leung, T. S., Lyon, S., Marrow, J., Ganther, W. and Cole, I. (2011). Atmospheric-induced stress corrosion cracking of austenitic stainless steels under limited chloride supply. Proc. 18th Int. Corros. Cong., Perth, Australia.

Dong, P., Hong, J. and Bouchard, P. (2005). Analysis of residual stresses at weld repairs. International Journal of Pressure Vessels and Piping 82, 258-269.

Dong, P., Zhang, J. and Bouchard, P. (2002). Effects of repair weld length on residual stress distribution. Journal of pressure vessel technology 124, 74-80.

Elcoate, C., Dennis, R., Bouchard, P. and Smith, M. (2005). Three dimensional multi-pass repair weld simulations. International Journal of Pressure Vessels and Piping 82, 244-257.

Enos, D. G., Bryan, C. R. and Norman, K. M. (2013). Data Report on Corrosion Testing of Stainless Steel SNF Storage Canisters, FCRD-UFD-2013-000324. U.S. Department of Energy, Office of Used Nuclear Fuel Disposition.

EPRI. (2011). Extended Storage Collaboration Program (ESCP) Progress Report and Review of Gap Analyses. Palo Alto, CA.

EPRI. (2014). Calvert Cliffs Stainless Steel Dry Storage Canister Inspection. Palo Alto, CA.

Gellrich, G. H. (2013). Response to Request for Additional Information, Re: Calvert Cliffs Independent Spent Fuel Storage Installation License Renewal Application (TAC No. L24475) dated April 24, 2013, NRC Adams accession numbers ML13119A242, ML13119A243, and ML13119A244.

George, D. and Smith, D. (2005). Through thickness measurement of residual stresses in a stainless steel cylinder containing shallow and deep weld repairs. International Journal of Pressure Vessels and Piping 82, 279-287.

Hanson, B., Alsaed, H., Stockman, C., Enos, D., Meyer, R. and Sorenson, K. (2012). Gap analysis to support extended storage of used nuclear fuel, FCRD-USED-2011-000136. U.S. Department of Energy.

Hayashibara, H., Mayuzumi, M. and Mizutani, Y. (2008). Effects of temperature and humidity on atmospheric stress corrosion cracking of 304 stainless steel. CORROSION 2008.

Hossain, M., Goudar, D., Truman, C. E. and Smith, D. J. (2011). Simulation and measurement of residual stresses in a type 316h stainless steel offset repair in a pipe girth weld. Materials Science Forum: Trans Tech Publ, 492-497.

Hossain, S., Truman, C., Smith, D. and Bouchard, P. (2006). Measurement of residual stresses in a type 316H stainless steel offset repair in a pipe girth weld. Journal of pressure vessel technology 128, 420-426.

Kain, R. M. (1990). Marine atmosphere corrosion cracking of austenic stainless steels. Materials Performance 29, 60-62.

Kosaki, A. (2008). Evaluation method of corrosion lifetime of conventional stainless steel canister under oceanic air environment. Nuclear Engineering and Design 238, 1233-1240.

Mahmoudi, A., Hossain, S., Truman, C., Smith, D. and Pavier, M. (2009). A new procedure to measure near yield residual stresses using the deep hole drilling technique. Experimental Mechanics 49, 595-604.

Mahmoudi, A., Truman, C., Smith, D. and Pavier, M. (2011). The effect of plasticity on the ability of the deep hole drilling technique to measure axisymmetric residual stress. International Journal of Mechanical Sciences 53, 978-988.

Mintz, T. S., Caseres, L., He, X., Dante, J., Oberson, G., Dunn, D. S. and Ahn, T. (2012). Atmospheric Salt Fog Testing to Evaluate Chloride-Induced Stress Corrosion Cracking of Type 304 Stainless Steel. Corrosion 2012. Salt Lake City, March 11-15: NACE.

Nakayama, G. (2006). Atmospheric stress corrosion cracking (ASCC) susceptibility of stainless alloys for metallic containers. In: VanIseghem, P. (ed.) Scientific Basis for Nuclear Waste Management XXIX, pp. 845-852.

Nakayama, G. and Sakakibara, Y. (2013). Prediction Model for Atmospheric Stress Corrosion Cracking of Stainless Steel. ECS Transactions 50, 303-311.

NRC. (2012a). Identification and Prioritization of the Technical Information Needs Affecting Potential Regulation of Extended Storage and Transportation of Spent Nuclear Fuel. Draft for comment. Washington, D.C. U.S. NRC.

NRC. (2012b). Potential Chloride Induced Stress Corrosion Cracking of Austenitic Stainless Steel and Maintenance of Dry Cask Storage System Canisters, NRC Information Notice 2012-20, November 14, 2012. Washington, D.C. U.S. NRC.

NRC. (2013). Finite Element Analysis of Weld Residual Stresses in Austenitic Stainless Steel Dry Cask Storage System Canisters, NRC Technical Letter Report (ADAMS ML13330A512). Washington D.C. Nuclear Regulatory Commission.

NWTRB. (2010). Evaluation of the technical basis for extended dry storage and transportation of used nuclear fuel. Arlington, VA. Nuclear Waste Technical Review Board.

Pacific Nuclear Fuel Services, I. (1991). Topical Report for the NUTECH Horizontal Modular Storage System for Irradiated Nuclear Fuel NUHOMS-24P, Document NUH-002 Rev. 2A, April 1991. Adams ML110730769.

Parrott, R. and Pitts, H. (2011). Chloride stress corrosion cracking in austenitic stainless steel: Assessing susceptibility and structural integrity. U.K. Health and Safety Executive.

Prosek, T., Iversen, A. and Taxén, C. (2009). Low temperature stress corrosion cracking of stainless steels in the atmosphere in presence of chloride deposits. Corrosion 65, 105-117.

Prosek, T., Le Gac, A., Thierry, D., Le Manchet, S., Lojewski, C., Fanica, A., Johansson, E., Canderyd, C., Dupoiron, F. and Snauwaert, T. (2014). Low temperature stress corrosion cracking of austenitic and duplex stainless steels under chloride deposits. Corrosion.

Tani, J. I., Mayuzurmi, M. and Hara, N. (2009). Initiation and propagation of stress corrosion cracking of stainless steel canister for concrete cask storage of spent nuclear fuel. Corrosion 65, 187-194.